

# Response of thermoluminescent dosimeters to photons simulated with the Monte Carlo method

M. Morales<sup>a,\*</sup>, C.C. Guimarães<sup>b</sup>, E. Okuno<sup>b</sup>

<sup>a</sup>*Centro do Reator de Pesquisas, Instituto de Pesquisas Energéticas e Nucleares, Caixa Postal 11049, CEP 05422-970, São Paulo, SP, Brazil*

<sup>b</sup>*Laboratório de Dosimetria, Instituto de Física da Universidade de São Paulo, Caixa Postal 66318, CEP 05315-970, São Paulo, SP, Brazil*

Received 8 October 2004; received in revised form 29 December 2004; accepted 18 January 2005  
Available online 31 March 2005

---

## Abstract

Personal monitors composed of thermoluminescent dosimeters (TLDs) made of natural fluorite ( $\text{CaF}_2\text{:NaCl}$ ) and lithium fluoride (Harshaw TLD-100) were exposed to gamma and X rays of different qualities. The GEANT4 radiation transport Monte Carlo toolkit was employed to calculate the energy depth deposition profile in the TLDs. X-ray spectra of the ISO/4037-1 narrow-spectrum series, with peak voltage (kVp) values in the range 20–300 kV, were obtained by simulating a X-ray Philips MG-450 tube associated with the recommended filters. A realistic photon distribution of a  $^{60}\text{Co}$  radiotherapy source was taken from results of Monte Carlo simulations found in the literature. Comparison between simulated and experimental results revealed that the attenuation of emitted light in the readout process of the fluorite dosimeter must be taken into account, while this effect is negligible for lithium fluoride. Differences between results obtained by heating the dosimeter from the irradiated side and from the opposite side allowed the determination of the light attenuation coefficient for  $\text{CaF}_2\text{:NaCl}$  (mass proportion 60:40) as  $2.2\text{ mm}^{-1}$ .

© 2005 Elsevier B.V. All rights reserved.

PACS: 87.66.Sq; 87.58.Sp; 87.64.Aa

Keywords: Thermoluminescence; Dosimeter; Monte Carlo; GEANT4

---

## 1. Introduction

Thermoluminescent materials are extensively used in personal and environmental dosimetry. Typical dosimeters used for X and  $\gamma$  radiation consist of small thermoluminescent detectors (TLDs), some of them associated with filters,

---

\*Corresponding author. Tel.: +55 11 38169181;  
fax: +55 11 38169188.

E-mail address: [morales@curiango.ipen.br](mailto:morales@curiango.ipen.br) (M. Morales).

placed together inside a badge. The dose determination begins from the readout process, which is performed by heating the TLD on a metallic planchet and detecting the emitted light with a photomultiplier tube (PMT). Transparency to its own emitted light is an important property of the TLD, since it permits the achievement of high efficiency in the thermoluminescence (TL) intensity measurement. Transparency is also important to avoid that non-homogeneous deposition of energy inside the TLD affects the readout process. Typical TLDs are made of elements with low atomic number and have thickness of the order of 1 mm. Due to these characteristics, the absorbed dose is practically homogeneous for photons with energies above 40 keV. However, for photons with lower energies, the absorbed dose in the region near the radiation incidence side of TLD is greater than near the opposite side. The non-homogeneity of the dose distribution affects the TL readout, depending on the transparency of the material and on the placement of the TLD relative to the PMT. The knowledge of the influence of light absorption on the readout process is important, since dosimeter calibrations are usually performed with photon beams which frequently present low-energy photons. The effect of transparency can be observed through the difference between the TL intensity obtained by heating the TLD from the irradiated side and from the opposite side. On the other hand, the energy depth deposition profile in the TLD can be calculated using analytical or Monte Carlo methods. The combination of the measured TLD response from both sides and an adequate theoretical model for the TLD response allows the determination of light attenuation in the TLD.

Dosimeters are mostly complex systems, formed by several materials with different geometric shapes and usually submitted to radiation with spectra of wide energy distribution. Due to this complexity, calculations of dose distribution with Monte Carlo methods are preferable to analytical methods. The capabilities of data processing of the new generations of personal computers allow the employment of the Monte Carlo method in simulations of complex physical systems. Solution of problems which involve the transport of

radiation in matter is an example where the Monte Carlo method has been applied with success in the last years, including simulations of TLDs [1]. This work presents an application of the Monte Carlo method to obtain the response of dosimeters used in personal monitoring. The detectors are composed by lithium fluoride and natural calcium fluoride (fluorite) TL crystals. Comparison of experimental and simulated results allowed the determination of the attenuation coefficient for self-absorption of light in the semi-transparent calcium fluoride detector. The simulations were performed with the GEANT4 toolkit [2,3], which was recently validated for simulations in low-energy medical physics [4] and also considered in a review article concerning Monte Carlo modelling of radiotherapy photon beams [5].

## 2. Experiment

Monitors used for personal dosimetry were exposed to X and gamma radiation using the facilities of the Dosimetry Laboratory of the Physics Institute of São Paulo University. Each monitor consists of a polyvinyl chloride (PVC) badge containing two LiF:Mg,Ti (Harshaw TLD-100) with dimensions of  $3.1 \times 3.1 \times 0.9 \text{ mm}^3$ , and two natural calcium fluoride ( $\text{CaF}_2$ ) detectors. Pellets of  $\text{CaF}_2\text{:NaCl}$  were prepared by mixing Brazilian natural  $\text{CaF}_2$  to NaCl, both in powder form, in weight proportion of 60–40%, followed by cold-pressing with a hydraulic press. Details about the annealing and characteristics of TLDs based on Brazilian fluorite are described elsewhere [6–8]. The pellets have a 5.00 mm diameter, average thickness and mass of 0.84 mm and 42 mg, respectively. Their average density is approximately  $2.52 \text{ g cm}^{-3}$ , which is about 6% less than the expected value for this compound ( $2.68 \text{ g cm}^{-3}$ ). This difference is due to the volume of air that remains between the powder grains. The detectors were packed with PVC films with thickness of  $0.027 \text{ g cm}^{-2}$ . A paper card with thickness of  $0.018 \text{ g cm}^{-2}$  is employed for the user identification. Since  $\text{CaF}_2$  and LiF have different sensitivity to low-energy photons, the ratio of the response of the detectors is a function of the

incident photon energy and is taken into account in the dose evaluation [8]. One of each type of detector is placed between a lead filter, but in this work, only data related to detectors without filter were used.

The radiation beams used in this study consisted of X rays produced by a Philips tube, model MG 450, and gamma rays emitted by a  $^{60}\text{Co}$  radiotherapy source (Picker X-Ray Corporation) with low activity (320 GBq at the time these studies were performed). The monitors were irradiated free-in-air with radiation qualities of the ISO narrow-spectrum series (N) [9]. Eight monitors were irradiated with beams of qualities N-20, N-25, N-30 and N-40 and four monitors with N-60, N-80, N-100, N-120, N-200, N-250 and N-300. The monitors were placed at a distance of 218 cm from the radiation source and were submitted to dose in the region of linear response, i.e. 5 mGy air kerma.

A TL reader built in the Physics Institute of São Paulo University [10], based on a SR400 photon counting system, was employed to measure the glow curves. In the readout process, both LiF and  $\text{CaF}_2$  were placed with the irradiated side in contact to the planchet for half of the detectors and with the opposite side for the other half. The results showed no differences other than statistical fluctuation for LiF, while the TL of  $\text{CaF}_2$  was more intense when the irradiated side faced the PMT, mainly for the low-energy beams. Visual inspection of the detectors indicates, in a rough way, that the obtained results are expected, since the LiF's TLD-100 are translucent while the pellets of  $\text{CaF}_2$  are white opaque. Previous studies of natural LiF detectors submitted to alpha particles [11] and synchrotron radiation [12] reported low values for the light attenuation coefficient. In this work, the self-absorption of thermoluminescence was analyzed only for the  $\text{CaF}_2$  detectors.

### 3. Simulation

The Monte Carlo calculations were performed using the GEANT4 toolkit [2,3] version 5.1p01 (release date: 19 May 2003). This package is written in C++ programming language and

provide the necessary tools to simulate the passage of radiation through matter. Although the GEANT project was formerly designed for high-energy and nuclear physics, the recent versions include a low-energy extension of electromagnetic processes, which is suitable to simulate the transport of electrons, positrons, photons and hadrons with energy values as low as 250 eV [4].

In this work, electromagnetic processes considered for photons were Rayleigh scattering, Compton scattering, photoelectric effect and pair production. Ionization, bremsstrahlung and multiple Coulomb scattering were considered for the interactions of electrons. All simulations were performed with the low-energy extension physics models. Two relevant parameters for the Monte Carlo calculation with GEANT4 are the cut in the step size and the cut in the energy for production of secondary particles. In GEANT4 the step size is chosen in length units and its correspondence in energy is presented for each material. Table 1 shows the energy values of the cuts used in this work. Cut for secondary particles was chosen to be 250 eV for all materials.

The simulations were performed in two steps: the first one for the calculation of the energy distribution of the radiation field and the second one for the calculation of the absorbed energy in the dosimeter. Description of each step follows below.

Table 1  
Energy values (keV) of cuts for all materials used in the Monte Carlo simulations

| Material       | Cut for photons | Cut for electrons |
|----------------|-----------------|-------------------|
| W              | 1.6             | 8.9               |
| Pb             | 1.2             | 4.5               |
| Sn             | 0.50            | 2.0               |
| Cu             | 0.50            | 4.2               |
| Al             | 0.50            | 0.81              |
| Be             | 0.25            | 0.50              |
| LiF            | 0.25            | 0.25              |
| $\text{CaF}_2$ | 0.25            | 1.0               |
| NaCl           | 0.25            | 0.57              |
| PVC            | 0.25            | 0.25              |
| Paper          | 0.25            | 0.25              |
| Air            | 0.25            | 0.25              |

### 3.1. Radiation field

#### 3.1.1. X-ray

The X-ray tube was simulated by impinging electrons on a tungsten target. The electron beam was directed at an angle of  $22^\circ$  with the normal of the target surface. Intrinsic filtration was simulated by placing a beryllium disc with thickness of 2.2 mm between the target and the region where the energy of the photon was registered. For each value of selected peak voltage (kVp), the spectrum of the photons was recorded in channels with width of 0.25 keV. The number of projectiles necessary to obtain good statistics depends on the kVp. A typical simulation for kVp = 100 kV was performed with  $5 \times 10^8$  projectiles, and calculation time was 35 h using a Pentium 4 processor with 2.4 GHz clock frequency.

The filtration of the generated spectrum was simulated by directing the photon beam to one or more discs made of Al, Cu, Sn and Pb with the thickness corresponding to that used in the experiment to obtain each radiation quality. The filtered spectrum was also recorded in channels with width of 0.25 keV. Twelve radiation qualities of the ISO/4037-1 narrow-series spectra [9] with effective energies in the range from 15 to 230 keV (N-20 to N-300) were simulated. Although dosimeters were not experimentally irradiated with the radiation quality N-150, the simulation was performed also for this spectrum.

As an example, Fig. 1(a) shows the energy spectrum of photons emitted from the target at an aperture angle of  $30^\circ$  obtained with electrons of 80 keV. Fig. 1(b) shows the N-80 spectrum, which is obtained after filtration with 2.0 mm of copper and 4.0 mm of aluminum. Table 2 presents a comparison between simulated and reference values for mean energy and resolution of the narrow-series spectra. Good agreement is observed for both quantities.

#### 3.1.2. Gamma radiation of $^{60}\text{Co}$ -source

The monitors were irradiated in the field of a  $^{60}\text{Co}$  radiotherapy source which is similar to that described in Ref. [13]. In the present work, the energy spectrum published by these authors (Table I of Ref. [13]) was used to simulate the  $^{60}\text{Co}$  source beam.

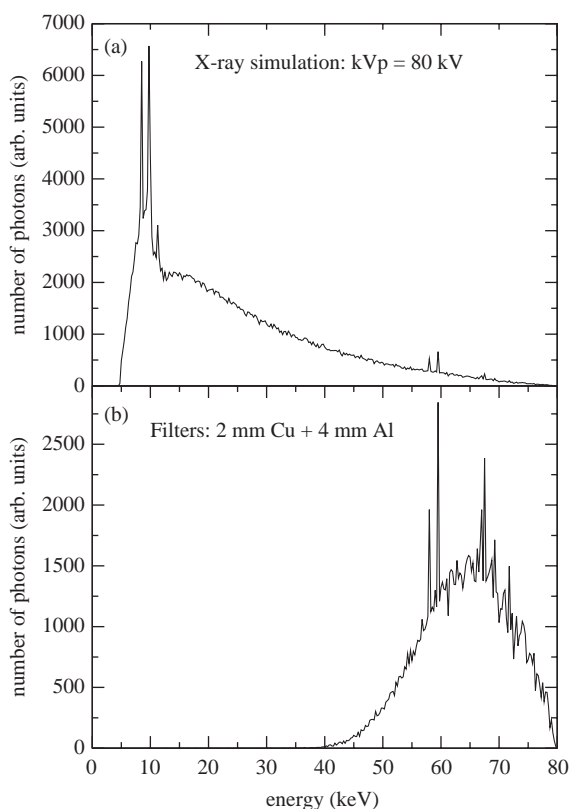


Fig. 1. X-ray spectra simulated with the Monte Carlo Method: (a) spectrum for kVp = 80 kV; (b) same spectrum after filtering with 2.0 mm copper and 4.0 mm aluminum.

### 3.2. Monitor

The simulated monitor was composed by two parallelepipeds of LiF and two discs of  $\text{CaF}_2:\text{NaCl}$  with dimensions corresponding to the real ones. In order to obtain the depth profile of the energy deposited in the  $\text{CaF}_2:\text{NaCl}$  detectors, they were segmented in ten slices, each one with thickness of 84  $\mu\text{m}$ .

The badge contained one sheet of paper with thickness of 0.20 mm placed in front of the detectors and two sheets of PVC with thickness of 0.22 mm, one placed in front of the paper sheet and the other one placed at the back side of the detectors. Density and chemical composition used were, respectively, 0.83  $\text{g cm}^{-3}$  and  $\text{C}_{10}\text{H}_{11}\text{O}_4$  for paper, 1.20  $\text{g cm}^{-3}$  and  $\text{C}_2\text{H}_3\text{Cl}$ , respectively, for PVC. The experiment was simulated by disposing

Table 2

Mean photon energy (keV) and resolution for narrow-series radiation qualities, as defined in Ref. [9]. Comparison between simulated (GEANT4) and tabulated (ISO-4037) values

| Radiation quality | Mean photon energy |                   | Difference (%) | Resolution(%) |          | Difference (%) |
|-------------------|--------------------|-------------------|----------------|---------------|----------|----------------|
|                   | GEANT4             | ISO-4037          |                | GEANT4        | ISO-4037 |                |
| N-20              | 15.9               | 16.4 <sup>a</sup> | 3.8            | 33.4          | 34       | 1.7            |
| N-25              | 19.9               | 20.4 <sup>a</sup> | 2.5            | 33.7          | 33       | 2.1            |
| N-30              | 24.2               | 24.7 <sup>a</sup> | 2.1            | 33.9          | 32       | 5.9            |
| N-40              | 32.8               | 33                | 0.7            | 30.2          | 30       | 0.7            |
| N-60              | 47.0               | 48                | 2.1            | 37.9          | 36       | 5.2            |
| N-80              | 64.0               | 65                | 1.5            | 32.3          | 32       | 1.1            |
| N-100             | 82.9               | 83                | 0.2            | 28.2          | 28       | 0.8            |
| N-120             | 99.3               | 100               | 0.7            | 28.0          | 27       | 3.9            |
| N-150             | 116.4              | 118               | 1.4            | 38.7          | 37       | 4.6            |
| N-200             | 163.0              | 164               | 0.6            | 29.9          | 30       | 0.2            |
| N-250             | 206.8              | 208               | 0.6            | 26.8          | 28       | 4.3            |
| N-300             | 249.4              | 250               | 0.2            | 27.2          | 27       | 0.6            |

<sup>a</sup>Value taken from the more recent ISO 4037—Part 4 [9].

the monitor inside a chamber filled with air, at a distance of 218 cm of a radiation point source. The radiation field consisted of a cone with aperture angle of  $0.70^\circ$ , which is enough to irradiate the whole monitor. Typical processing time for the simulation of irradiation with N-100 radiation quality was 1900 s.

#### 4. Results

The results of the energy absorbed in the dosimeters obtained in the simulations showed a non-uniform distribution for radiation beams of low energies. Fig. 2 shows the logarithm of the energy absorbed in each slice of the fluorite detector for four radiation qualities. In order to calculate the self-absorption of light in the fluorite detector, the light attenuation in the reading process of the  $\text{CaF}_2:\text{NaCl}$  was considered to have an exponential dependence with the thickness of material, following the Lambert's Law. Since in the simulations the TL intensity is assumed to be proportional to the energy deposited in the detector, the effect of the light attenuation can be obtained by applying an exponential attenuation in the energy deposited in the pellet as a function of the thickness of material that the light

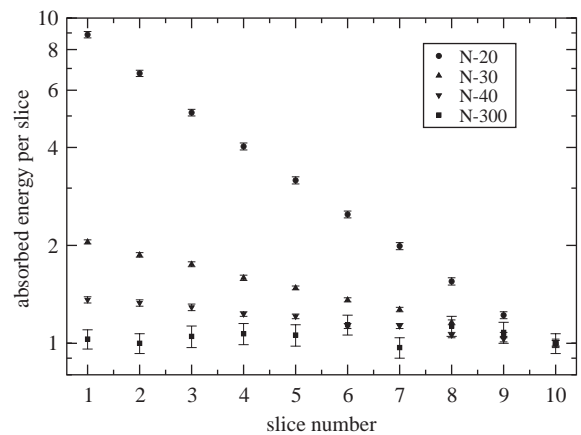


Fig. 2. Absorbed energy per slice of fluorite for radiation of qualities N-20, N-30, N-40 and N-300. The first slice corresponds to the irradiated side. Vertical axis is normalized to the energy absorbed in the 10th slice. Slice thickness:  $84\ \mu\text{m}$ .

traverses. It was considered that the absorbed energy  $E_{0i}$  in each slice  $i$  of the  $\text{CaF}_2:\text{NaCl}$  pellet calculated with the Monte Carlo method was attenuated to  $E_{Ai}$ , according to the expression

$$E_{Ai} = E_{0i} \exp(-\mu x_i) \quad (1)$$

where  $\mu$  is the light attenuation coefficient of TL in  $\text{CaF}_2:\text{NaCl}$  and  $x_i$  is the distance of the center of the slice  $i$  to the side of the dosimeter which faces

the PMT. In the present simulation, with the  $\text{CaF}_2\text{:NaCl}$  pellet segmented in ten slices, the total TL intensity is obtained by summing the attenuated contributions of each slice. The calculation of the TL intensity for read-out from the irradiated side facing the PMT is given by

$$\text{TL(irradiated)} = K \sum_{i=0}^{n-1} E_{0i} \exp \left[ -\mu \left( \frac{d}{2} + id \right) \right] \quad (2)$$

and for readout from the side opposite to irradiation by

$$\text{TL(opposite)} = K \sum_{i=0}^{n-1} E_{0i} \times \exp \left[ -\mu \left( \frac{d}{2} + (n-1-i)d \right) \right]. \quad (3)$$

In these expressions  $K$  is a constant,  $n$  is the number of slices and  $d$  is the thickness of each slice. Figs. 3(a) and (b) show the scheme of the readout process from the irradiated side and from the opposite side, respectively. The dependence of the TL self-absorption on the effective energy of the irradiation field for the TLDs is presented in Fig. 4. The vertical axis represents the ratio of TL intensity for readout with the PMT facing the irradiated side over the readout from the opposite side. The experimental data of Fig. 4 show a

strong dependence of the TL intensity on the side of the dosimeter which is facing the PMT for photon effective energies below 46 keV. When the PMT is facing the irradiated side, the TL intensity is two times higher than when it is facing the opposite side for effective energy of 15 keV. For effective energies above 46 keV, the energy deposition in the dosimeter is homogeneous and the observed differences are comparable to the experimental errors. In Fig. 4, calculated values obtained from the simulated absorbed energies and Eqs. (2) and (3) using attenuation coefficients from 1.2 to  $3.6 \text{ mm}^{-1}$  are also presented. The value of

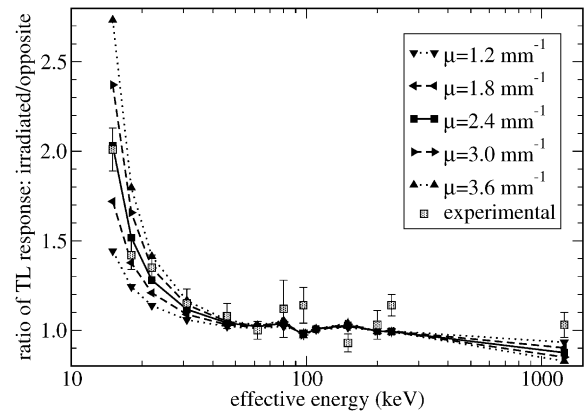


Fig. 4. Thermoluminescence response of fluorite dosimeters: ratio of readout from the irradiated side over readout from the opposite side as a function of photon effective energy.

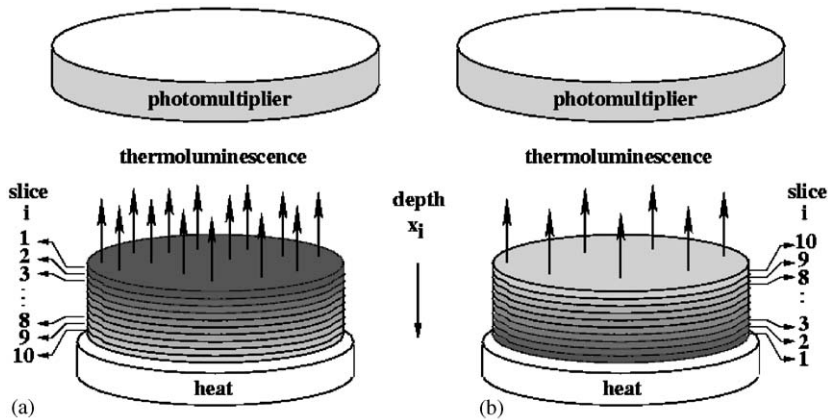


Fig. 3. Scheme of the thermoluminescence read-out process: (a) with the irradiated side and (b) with the side opposite to irradiation facing the photomultiplier tube.



$\mu = 2.20(25)\text{mm}^{-1}$  was obtained with the least-squares method as the one which better fits the experimental data.

It is worthy to mention that Eqs. (2) and (3) do not include contribution from reflection of light on the metallic planchet. Ipe et al. [12] used the same approximation to model the response of LiF TLDs, based on measurements that indicate the negligible influence of the reflection on the TLD response modelling. In fact, the inclusion of reflection contribution by changing Eqs. (2) and (3) showed no effect on the calculated value of the attenuation coefficient. The results are insensible to the reflection influence due to the large uncertainty in the experimental data (see Fig. 4).

The relative TL response of LiF and  $\text{CaF}_2\text{:NaCl}$  detectors at different energies are very important to obtain the energy dependence of the dosimeter response. Figs. 5 and 6 show the ratio of TL response of  $\text{CaF}_2\text{:NaCl}$  over LiF for the irradiated and opposite side readout, respectively, as a function of the photon effective energy. The simulated data were calculated with the attenuation coefficient of  $2.2\text{mm}^{-1}$ . Good agreement between calculated and experimental results is observed.

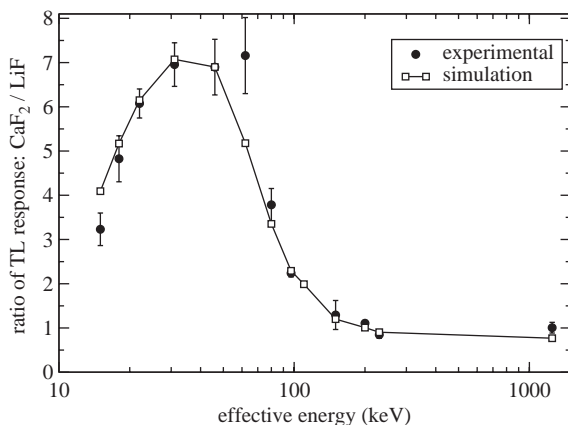


Fig. 5. Ratio of thermoluminescence response of fluorite dosimeters readout from the irradiated side over response of LiF dosimeters as a function of photon effective energy. The vertical axis was normalized to the energy of gamma rays of  $^{60}\text{Co}$ .

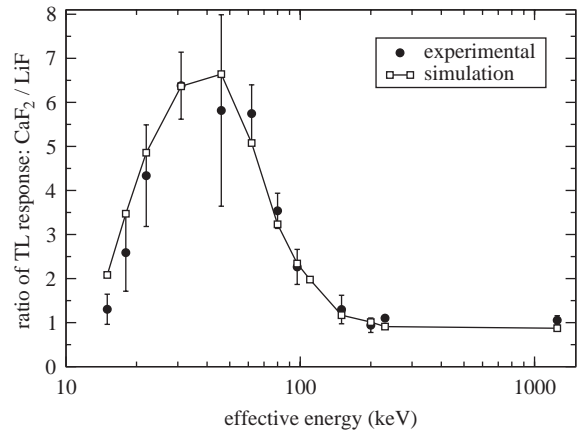


Fig. 6. Ratio of thermoluminescence response of fluorite dosimeters readout from the side opposite to irradiation over response of LiF dosimeters as a function of photon effective energy. The vertical axis was normalized to the energy of gamma rays of  $^{60}\text{Co}$ .

## 5. Conclusion

The TL response of  $\text{CaF}_2\text{:NaCl}$  and LiF detectors, used in personal monitoring, were analyzed by comparing the TL intensities obtained with the irradiated side facing the photomultiplier and with the side opposite to irradiation facing the photomultiplier. Differences observed for irradiation with low-energy photons revealed that the self-absorption of the light in  $\text{CaF}_2\text{:NaCl}$  is significative.

Comparison of experimental results with calculations of the absorbed dose obtained with the Monte Carlo method allowed the determination of the light attenuation coefficient in  $\text{CaF}_2\text{:NaCl}$  pellet as  $2.2\text{mm}^{-1}$ . This value depends on an adequate description of the dosimeter geometry and electromagnetic physics models employed by the simulation code. The recent releases of GEANT4 provide tools which are well suited to these requirements.

## Acknowledgements

One of the authors, C.C. Guimarães, thanks the financial support given by CAPES (Coordenação

de Aperfeiçoamento de Pessoal de Nível Superior, Brazil).

## References

- [1] H. Jung, K.J. Lee, J.-L. Kim, S.-Y. Lee, *Rad. Meas.* 38 (2004) 71.
- [2] S. Agostinelli, et al., *Nucl. Instr. and Meth. A* 506 (2003) 250.
- [3] GEANT4 Web page: <http://cern.ch/geant4>.
- [4] J.-F. Carrier, L. Archambault, L. Beaulieu, *Med. Phys.* 31 (2004) 484.
- [5] F. Verhaegen, J. Seuntjens, *Phys. Med. Biol.* 48 (2003) R107.
- [6] P. Trzesniak, E.M. Yoshimura, M.T. Cruz, E. Okuno, *Radiat. Prot. Dosim.* 34 (1990) 167.
- [7] E. Okuno, S. Owaki, T. Yamamoto, J.F.D. Chubaci, K. Inabe, Y. Fukuda, *Radiat. Prot. Dosim.* 47 (1993) 99.
- [8] C.C. Guimarães, E. Okuno, *Rad. Meas.* 37 (2003) 127.
- [9] International Organization for Standardization, X and gamma reference radiation for calibrating dosimeters and doserate meters and for determining their response as a function of photon energy. Part 1: Radiation characteristics and production methods. ISO 4037-1, First edition (15-12-1996). Part 4: Calibration of area and personal dosimeters in low energy X reference radiation fields, First edition (10-06-2004).
- [10] M.P. Diaz, N.K. Umisedo, E.M. Yoshimura, E. Okuno, in: *Proceedings of Encontro Anual de Física da Matéria Condensada*, Brazilian Physics Society, Brazil, 1994, p. 67.
- [11] P. Bilski, P. Olko, B. Burgkhardt, E. Piesh, M.P.R. Waligóorski, *Radiat. Prot. Dosim.* 55 (1994) 31.
- [12] N.E. Ipe, A. Fassò, K.R. Kase, R. Kaur, P. Bilski, P. Olko, *Radiat. Prot. Dosim.* 84 (1999) 169.
- [13] G.M. Mora, A. Maio, D.W.O. Rogers, *Med. Phys.* 26 (1999) 2494.